

Electronic Supplementary Information

S1. DFT calculations of organic molecules for the surface modification of silicon nanoparticles.

First, the optimum structures of Sty, Dec, and Nap were calculated by the DFT method (B3LYP/6-31G*). Molecular orbitals (MOs) and MO energy diagrams are shown in Figure S1-S3. Electronic absorption spectra were calculated for the optimum structures using the TD-DFT (B3LYP/6-31G*) method. The spectral characteristics were reproduced by these calculations (Table S1-S3), whereas the excitation energies were overestimated.

The lowest excited states of Sty are composed of (HOMO-1 \rightarrow LUMO) and (HOMO \rightarrow LUMO+1) electronic configurations, which can be often seen in the electronic states of benzene derivatives (Table S1, Figure S1).^{S1} Because of the small energy difference between the (HOMO-1 \rightarrow LUMO) and (HOMO \rightarrow LUMO+1) configurations ($\Delta E = 0.14$ eV), the (HOMO \rightarrow LUMO+1) configuration is heavily admixed with the (HOMO-1 \rightarrow LUMO) configuration, which results in the weak $S_0 \rightarrow S_1$ band (Table S1). To extend the π -conjugation length from Sty to Nap, the $S_0 \rightarrow S_1$ band shifted to the red-side (Table S3, Figure S3) because of the small HOMO-LUMO gap (Sty: 5.20 eV, Nap: 4.34 eV). The lowest excited states of Nap are composed of (HOMO \rightarrow LUMO) and (HOMO-1 \rightarrow LUMO) electronic configurations. Since the energy difference between the (HOMO \rightarrow LUMO) and (HOMO-1 \rightarrow LUMO) configurations is relatively large ($\Delta E = 0.64$ eV), the $S_0 \rightarrow S_1$ transition mainly originate from the (HOMO \rightarrow LUMO), which results in the relatively intense $S_0 \rightarrow S_1$ band. S_1 state of

Dec was expressed as a single electronic configuration (HOMO \rightarrow LUMO) (Table S2, Figure S2), whose energy is higher than the extended π -conjugated molecule such as Sty and Nap.

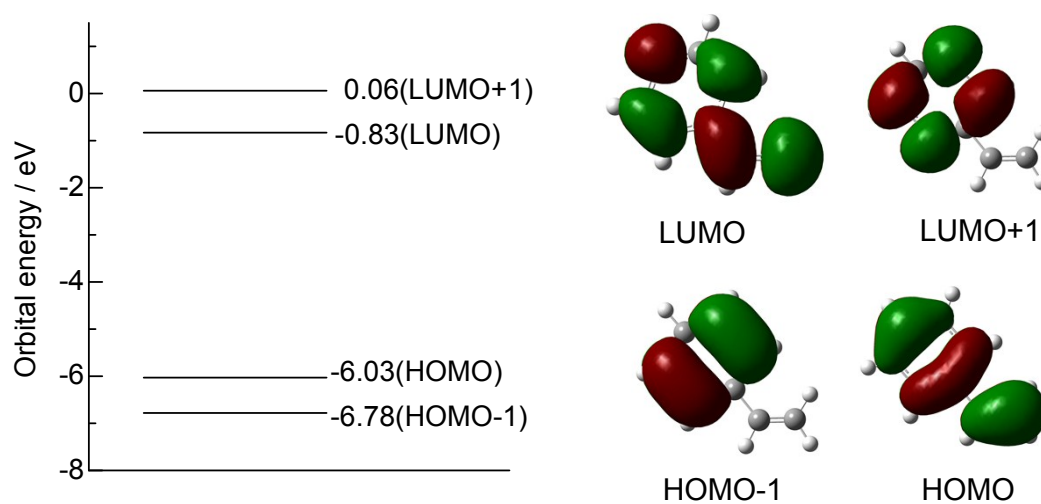


Figure S1. MOs and MO energy diagram of Sty.

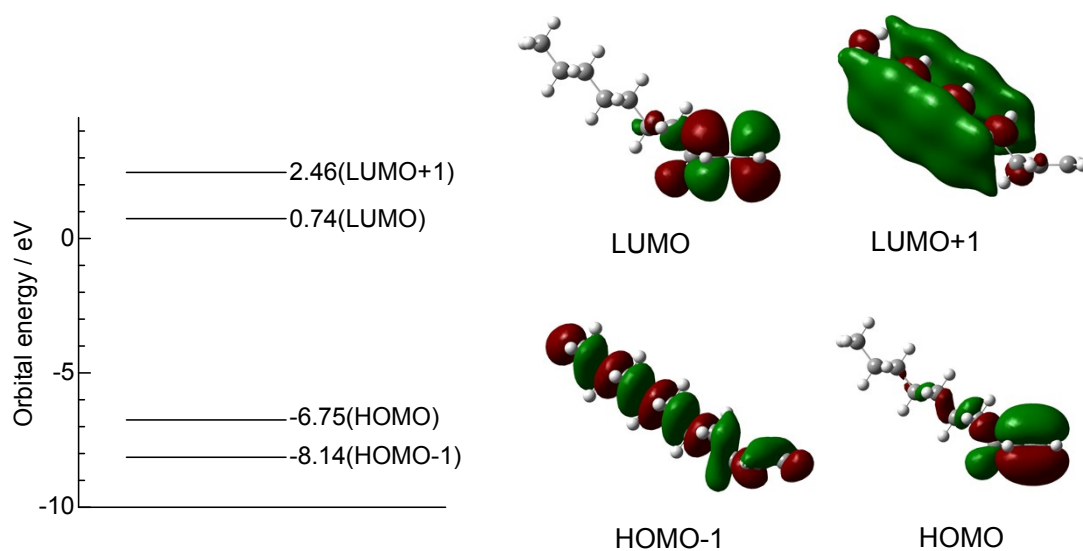


Figure S2. MOs and energy diagram of Dec.

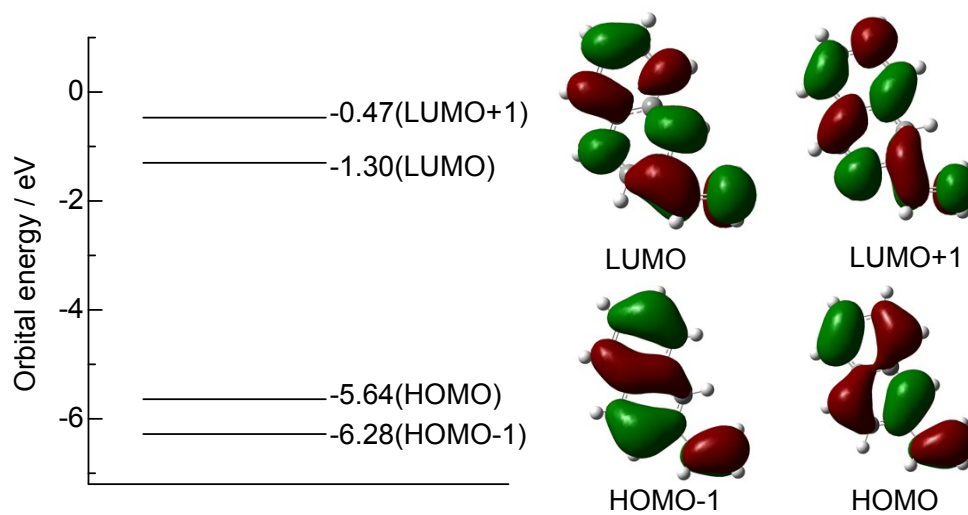


Figure S3. MOs and MO energy diagram of Nap.

Table S1. Calculation of the excited states for Sty.

	λ/nm	f	Main Configurations
S ₁	252	0.0273	H-1→L (48%), H→L+1 (43%)
S ₂	242	0.3622	H→L (88%)
S ₃	206	0.1911	H-1→L (38%), H→L+1 (52%)

Table S2. Calculation of the excited states for Dec.

	λ/nm	f	Main Configurations
S ₁	161	0.5450	H→L (84%), H-1→L (11%)
S ₂	153	0.0401	H-1→L (54%), H-7→L (17%)

Table S3. Calculation of the excited states for Nap.

	λ/nm	f	Main Configurations
S ₁	307	0.0825	H→L (85%), H-1→L (9%)

S ₂	300	0.0283	H-1→L (47%), H→L+1 (9%)
S ₃	240	1.0089	H→L (41%), H→L+1 (52%)

S2. DFT calculations for Silicon-cluster-Sty.

First, the optimum structures of Si-cluster-Sty (Figure S4, B3LYP/6-31G*). MOs are shown in Figure S5. The excited states properties were calculated for the optimum structure using the TD-DFT (B3LYP/6-31G*) method.

Calculated low energy bands were originating from the charge transfer (CT) transitions between Sty and Silicon cluster (Table S4). These oscillator strengths are much stronger than that of direct band gap transitions of silicon nanoparticles.^{S2} These results support that the red-shifted broad bands (Figure 5, Si-Sty and Si-Nap) is originating from the CT transitions between aromatic organic compounds and silicon nanoparticles.

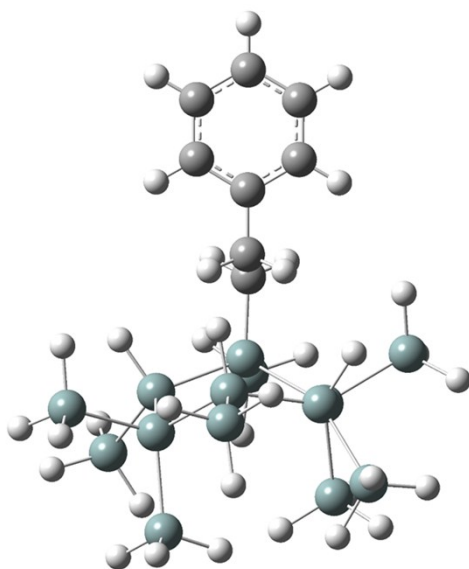


Figure S4. Molecular structure Si-cluster-Sty (C₈H₃₆Si₁₄).

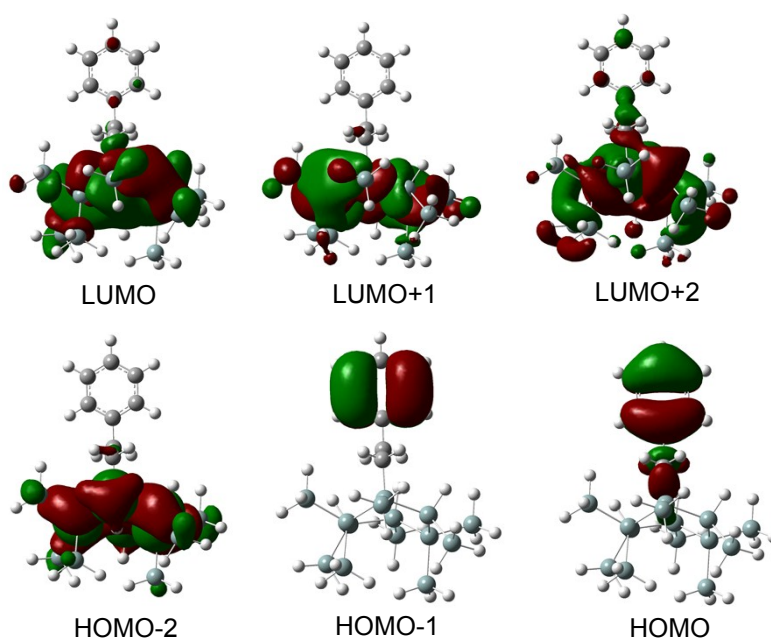


Figure S5. MOs of Si-cluster-Sty.

Table S4. Calculation of the excited states for Si-cluster-Sty.

	λ/nm	f	Main Configurations
S ₁	240	0.0432	H→L (99%)
S ₂	233	0.0021	H→L+1 (56%), H-1→L (16%)
S ₃	232	0.0008	H→L+1 (43%), H-1→L (25%)
S ₄	227	0.0397	H→L+2 (96%)
S ₅	225	0.0017	H-1→L (96%)

S3. Luminescence spectral changes of surface-modified silicon nanoparticles.

Freshly prepared samples were stored for four days in a cool dark place, and these luminescence spectra were measured. As time proceeds, the red luminescence band of silicon nanoparticle was scarcely red-shift and broadened (Figure S6, Si-Sty (after 4 days): 692 nm \rightarrow 721 nm, FWHM: 3880 cm^{-1} \rightarrow 3990 cm^{-1}).

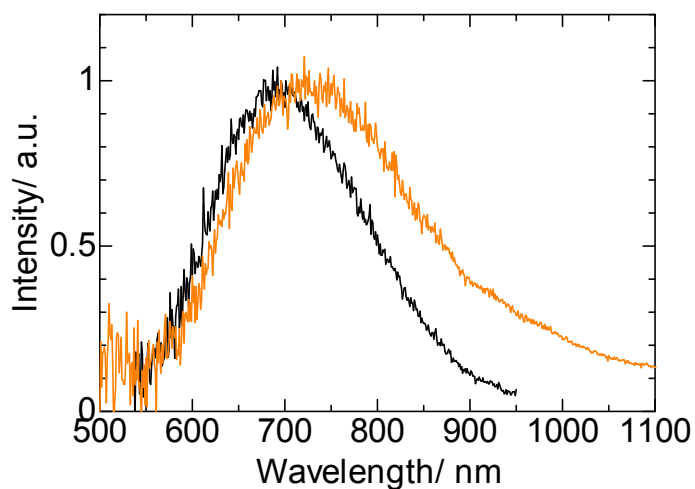


Figure S6. Luminescence spectra of Si-Sty (freshly prepared sample: black line, after four days: orange line). The spectra were normalized at the intense maxima.

S4. Luminescence spectrum change of Si-Nap depending on an excitation wavelength.

In the cases of Si-Sty and Si-Dec, the red-luminescence originating from silicon nanoparticles were clearly observed, which was independent on the excitation wavelength ($\lambda_{\text{ex}} = 260, 380 \text{ nm}$). However, in the case of Si-Nap excited by light at 260 nm, we found the intense luminescence originating from organic moieties ($\lambda_{\text{em}} = 326, 340, 355 \text{ nm}$) or their excimer (416 nm) on the silicon surface (Figure S7). These differences may originate from the larger radiation rates because of the larger transition dipole moment of the Nap moiety ($\pi-\pi^*$).

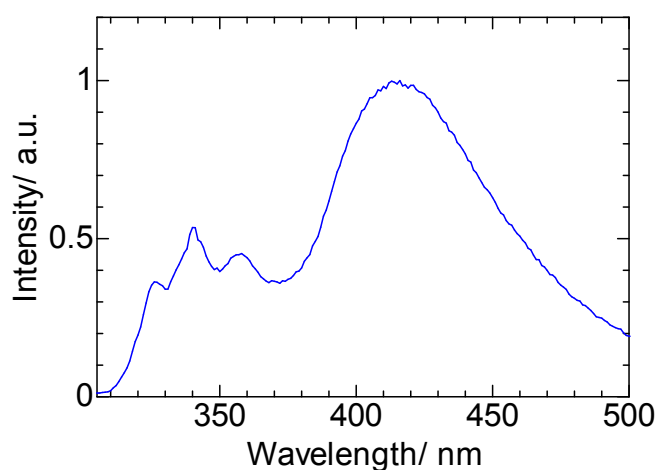


Figure S7. Luminescence spectrum of Si-Nap ($\lambda_{\text{ex}} = 260 \text{ nm}$). The spectrum was normalized at the intense maxima.

S5. Luminescence data for the old sample

We prepared the Sty-Si showing red-luminescence as the same method more than two years ago.^{S3} The sample has been stocked in the dark place at room temperature. We checked the sample showing still red-luminescence (Figure S8).

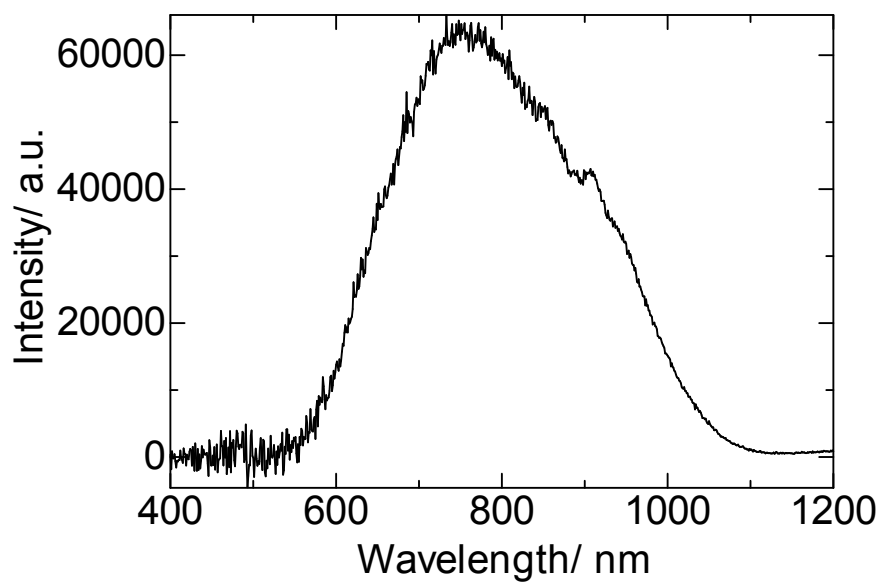


Figure S8. Luminescence spectrum of Si-Sty ($\lambda_{\text{ex}} = 260$ nm).

S6. Dynamic light scattering data for Sty-Si

Prepared Si-Sty was characterized using dynamic light scattering (DLS, BECKMAN COULTER DelsaNanoHC.) measurements. These size distributions are shown in Figure S9. Distributions of Si-Sty was also observed at around 3.7 nm (average size).

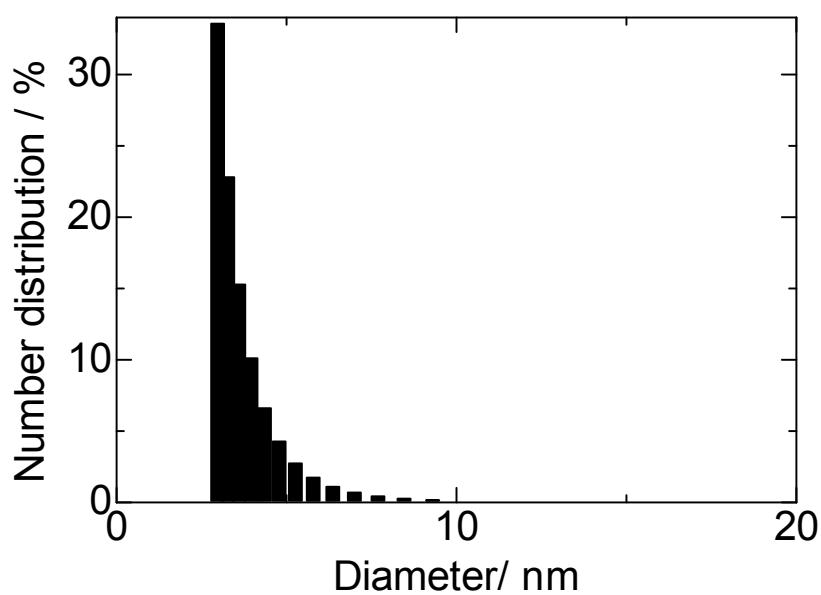


Figure S9. Size distribution of Si-Sty using DLS measurement.

S7. Luminescence decay profiles

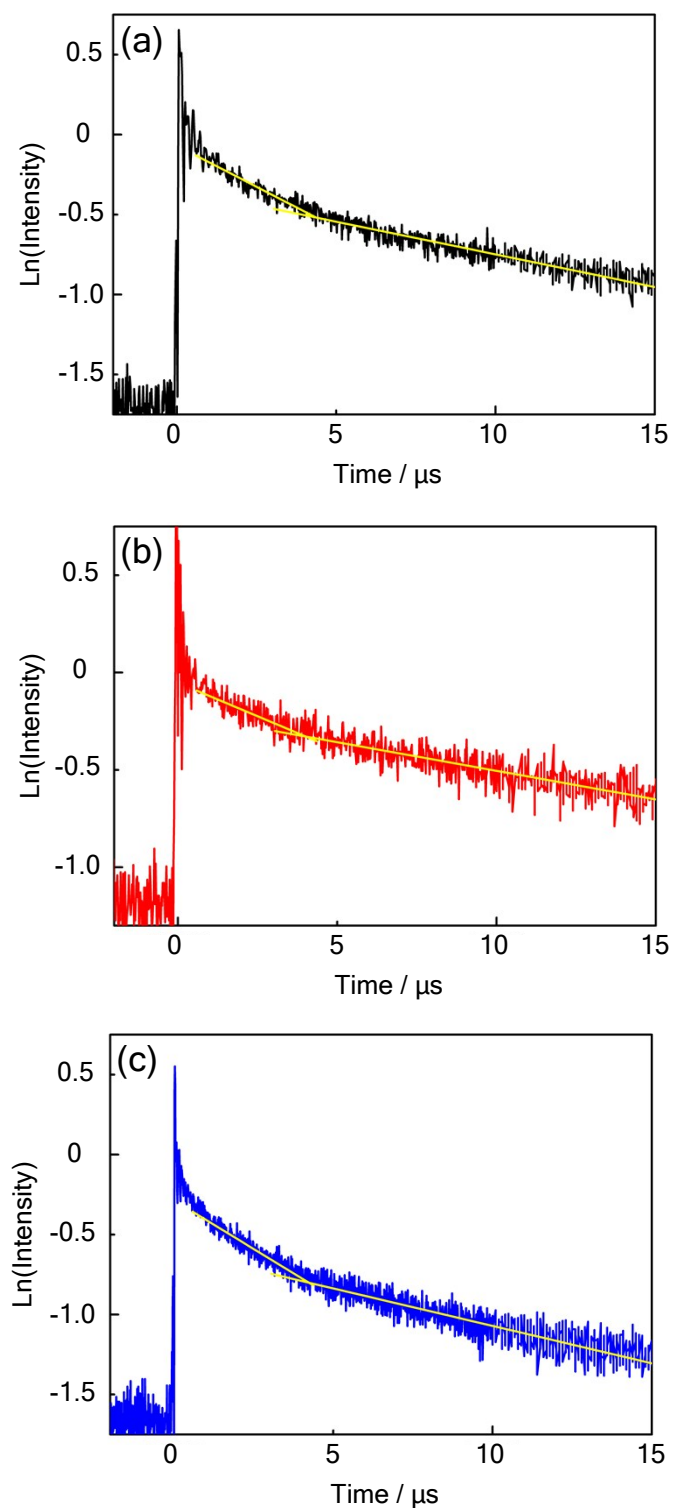


Figure S10. Luminescence decay profiles of Si-Sty (a), Si-Dec (b), and Si-Nap (c).

References

- [S1] C. Meier, A. Gondorf, S. Lüttjohann, A. Lorke and H. Wiggers, Silicon Nanoparticles: Absorption, Emission, and the Nature of the Electronic Bandgap, *J. Appl. Phys.*, 2007, **101**, 103112.
- [S2] A. L. Sklar, Rev. Electronic Absorption Spectra of Benzene and Its Derivatives, *Mod. Phys.*, 1942, **14**, 232.
- [S3] M. Miyano, S. Endo, H. Takenouchi, S. Nakamura, Y. Iwabuti, O. Shiino, T. Nakanishi and Y. Hasegawa, Novel Synthesis and Effective Surface Protection of Air-Stable Luminescent Silicon Nanoparticles, *J. Phys. Chem. C*, 2014, **118**, 19778-19784.